# (Tetrabenzoporphyrinato)nickel(II) Iodide. A Doubly Mixed Valence Molecular Conductor

**Jens Martinsen, Laurel J. Pace, Terry E. Phillips, Brian M. Hoffman,* and James A. Ibers***

*Contribution from the Department of Chemistry and Materials Research Center, Northwestern University, Evanston, Illinois 60201.* *Received April 1, 1981*

**Abstract:** We report a structural, magnetic, and charge-transport study of the new "molecular metal" produced by the iodine oxidation of (tetrabenzoporphyrinato)nickel(II), Ni(TBP). The compound is of composition $Ni(TBP)I_{1.0}$ and crystallizes in space group $D_{4h}^2$–$P4/mcc$ of the tetragonal system with two formula units in a cell of dimensions $a$ = 14.081 (25) Å and $c$ = 6.434 (11) Å at 113 K. Full-matrix least-squares refinement of 65 variables gave a final value of the conventional $R$ index on $F^2$ of 0.122 for 954 unique reflections. The crystal structure consists of planar Ni(TBP) units stacked metal-over-metal with a Ni–Ni spacing of 3.217 (5) Å at 116 K and with the units staggered by 41°. Running parallel to these stacks are chains of disordered $I_3^-$ ions. Their existence requires a mixed valency (partially oxidized) formulation whose average charge, or ionicity, of 0.33 may be represented by writing $[Ni(TBP)]^{0.33+}(I_3^-)_{1/3}$. Both structure and formulation of this new compound are the same as we recently found for (phthalocyaninato)nickel(II) iodide, Ni(Pc)I. The complex Ni(TBP)I has a room temperature conductivity of ca. 330 S cm$^{-1}$, which rises to a maximum of 600 S cm$^{-1}$ at ca. 95 K and decreases in an activated fashion at lower temperatures. The susceptibility is Pauli-like, being low (ca. 0.1 spins/Ni(TBP)) and roughly temperature independent above 100 K. However, the carrier spin $g$ values and line widths are anomalous; both are unusually large at room temperature ($g_{av}$ = 2.03, $\Gamma$ = 105 G) and increase strongly as the temperature is lowered. These observations lead us to conclude that this conductive molecular crystal exhibits a novel, doubly mixed valence state. Intermolecular mixed valency along a Ni(TBP) stack may be made explicit by writing the stoichiometric formula as $[Ni(TBP)]_2[Ni(TBP)]^+(I_3^-)$. In addition, there is a rapid interconversion between ligand and metal-oxidized electronic tautomers: $[Ni^{II}(TBP)^+] \rightleftharpoons [Ni^{III}(TBP)]$.

We have recently reported several studies on highly conducting quasi one-dimensional molecular solids whose metallomacrocycle building blocks may be viewed as variants on the porphine skeleton.[1-7] They show that, like the "organic metals",[8,9] molecular solids composed of transition-metal complexes can attain high electrical conductivity if the conducting subunits are essentially planar, crystallize as face-to-face stacks or chains, and adopt a nonintegral oxidation state. The last condition is usually attained by partial oxidation of a complex having an integral oxidation state.

Beyond these broad guidelines, however, there is still only a limited understanding of the correspondence between the properties of conducting molecular solids and the steric and electronic properties of the building blocks. Such information can only be obtained via a systematic correlation of solid-state characteristics with the geometric and electronic properties of the parent molecules. However, substantial modifications of the subunit electronic properties are generally accompanied by crystal structure changes or by alterations in the degree of partial charge transfer (ionicity). For example, the tetracyanoplatinate salts (TCP),[8,10] though subject to extensive off-stack variations of the counterion and the degree of hydration, are not amenable to modifications of the subunits. The organic metals offer a wider range of chemical flexibility;[8,9] however, in many instances, apparently small changes in the subunit lead to radical changes in the crystal structure[11a] and the degree of charge transfer or both.[11b] Nevertheless, several significant correlations have been reported. Subtle, off-stack effects on the properties of TTF salts have been observed through a systematic variation of the closed-shell anion.[12] On-stack variations in isostructural compounds have been achieved with solid solutions of the form $(TTF)_{1-x}(TSeF)_xA$, where A is either TCNQ[13a,b] or 2,5-diethyl-TCNQ and $0 \le x \le 1$. However, the ionicity (charge transfer) and also the one dimensionality are altered by the substitution of selenium for sulfur. Somewhat analogously, systematic explicit correlations between physical properties and ionicity have been obtained with solid solutions of

(1) (a) Peterson, J. L.; Schramm, C. J.; Stojakovic, D. R.; Hoffman, B. M.; Marks, T. J. *J. Am. Chem. Soc.* **1977**, *99*, 286–288. (b) Schramm, C. J.; Stojakovic, D. R.; Hoffman, B. M.; Marks, T. J. *Science (Washington, DC)* **1978**, *200*, 47–48. (c) Schramm, C. J.; Scaringe, R. P.; Stojakovic, D. R.; Hoffman, B. M.; Ibers, J. A.; Marks, T. J. *J. Am. Chem. Soc.* **1980**, *102*, 6702–6713.

(2) (a) Phillips, T. E.; Hoffman, B. M. *J. Am. Chem. Soc.* **1977**, *99*, 7734–7736. (b) Phillips, T. E.; Scaringe, R. P.; Hoffman, B. M.; Ibers, J. A. *J. Am. Chem. Soc.* **1980**, *102*, 3435–3444.

(3) Hoffman, B. M.; Phillips, T. E.; Soos, Z. G. *Solid State Commun.* **1980**, *33*, 51–54.

(4) Wright, S. K.; Schramm, C. J.; Phillips, T. E.; Scholler, D. M.; Hoffman, B. M. *Synth. Met.* **1979/1980**, *1*, 43–51.

(5) Hoffman, B. M.; Phillips, T. E.; Schramm, C. J.; Wright, S. K. In "Molecular Metals"; Hatfield, W. E., Ed.; Plenum Press: New York, 1979; pp 393–398.

(6) Euler, W. B.; Schramm, C. J.; Hoffman, B. M., manuscript in preparation.

(7) Pace, L. J.; Martinsen, J.; Ulman, A.; Hoffman, B. M.; Ibers, J. A.; manuscript in preparation.

(8) (a) Miller, J. S., Epstein, A. J., Eds. *Ann. N.Y. Acad. Sci.* **1978**, *313*. (b) Keller, H. J., Ed. "Chemistry and Physics of One-Dimensional Metals"; Plenum Press: New York, 1977. (c) Miller, J. S.; Epstein, A. J. *Prog. Inorg. Chem.* **1976**, *20*, 1–151. (d) Keller, H. J., Ed. "Low-Dimensional Cooperative Phenomena"; Plenum Press: New York, 1975. (e) Hatfield, W. E., Ed. "Molecular Metals"; Plenum Press: New York, 1979. (f) Devreese, J. T., Evrard, R. P., Van Doren, V. E., Eds. "Highly Conducting One-Dimensional Solids"; Plenum Press: New York, 1979. (g) Berlinsky, A. J. *Contemp. Phys.* **1976**, *17*, 331–354. (h) Barišič, S.; Bjeliš, A.; Cooper, J. R.; Leontić, B. "Quasi One-Dimensional Conductors I", *Lect. Notes Phys.* **1979**, *95*. (i) Barišič, S.; Bjeliš, A.; Cooper, J. R.; Leontić, B. *Ibid.* **1979**, *96*.

(9) (a) Soos, Z. G. *Annu. Rev. Phys. Chem.* **1974**, *25*, 121–153. (b) Soos, Z. G., Klein, D. J. "Molecular Association"; Foster, R., Ed.; Academic Press: New York, 1979; Vol. 1, pp 1–119. (c) Andrē, J. J.; Bieber, A.; Gautier, F. *Ann. Phys. (Paris)* **1976**, *1*, 145–256. (d) Torrance, J. B. In ref 8a, pp 210–233. (e) Torrance, J. B. *Acc. Chem. Res.* **1979**, *12*, 79–86.

(10) Abbreivations used: TCP, tetracyanoplatinates; TCNQ, tetracyanoquinodimethane; TTF, tetrathiafulvalene; TSeF, tetraselenafulvalene; NMP, *N*-methylphenazinium; Phen, phenazinium; OMTBP, 1,4,5,8,9,12,13,16-octamethyltetrabenzoporphyrin; TTT, tetrathiatetracene; HMTSF, hexamethylenetetraselenafulvalene; KCP, $K_2[Pt(CN)_4]Br_{0.3}\cdot 3H_2O$.

(11) (a) Kistenmacher, T. J. In ref 8a, pp 333–342. (b) Torrance, J. B.; Mayerle, J. J.; Bechgaard, K.; Silverman, B. D.; Tomkiewicz, Y. *Phys. Rev. B* **1980**, *22*, 4960–4965.

(12) (a) Wudl, F.; Schafer, D. E.; Walsh, W. M., Jr.; Rupp, L. W.; DiSalvo, F. J.; Waszczak, J. V.; Kaplan, M. L.; Thomas, G. A. *J. Chem. Phys.* **1977**, *66*, 377–385. (b) Somoano, R. B.; Gupta, A.; Hadek, V.; Datta, T.; Jones, M.; Deck, R.; Hermann, A. M. *Ibid.* **1975**, *63*, 4970–4976.

(13) (a) Engler, E. M.; Patel, V. V.; Andersen, J. R.; Tomkiewicz, Y.; Craven, R. A.; Scott, B. A.; Etemad, S. In ref 8a, pp 343–354. (b) Schultz, T. D.; Craven, R. A. In ref 8f, pp 147–225. (c) Andersen, J. R.; Craven, R. A.; Weidenborner, J. E.; Engler, E. M. *J. Chem. Soc., Chem. Commun.* **1977**, 526–527.

0002-7863/82/1504-0083$01.25/0 

the composition $(NMP)_{1-x}(Phen)_x(TCNQ)$,[10,14a] $0 \leq x \leq 1$, as well as with the pair of compounds, HMTSF–TCNQ and HMTSF–$TCNQF_4$.[14b-e]

In this paper, we show that the chemical flexibility inherent in the porphyrin-like metallomacrocycles as building blocks provides a unique opportunity to vary purely electronic properties of the subunits without any resultant steric or structural changes. We report a structural, magnetic, and charge-transport study of Ni(TBP)I, a highly conducting material obtained by partial oxidation of (tetrabenzoporphyrinato)nickel(II) (Ni(TBP)) with elemental iodine. We recently performed a similar study on the

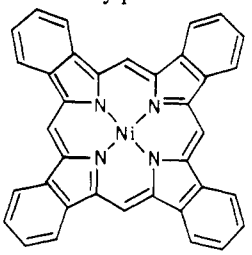

"molecular metal" Ni(Pc)I,[1] prepared from (phthalocyaninato)nickel(II) (Ni(Pc)), a complex which may be viewed as a Ni(TBP) analogue with four bridging nitrogen atoms replacing the methine carbon atoms. The electronic properties of the two Ni(L) parent molecules differ substantially.[15] Nevertheless, we find that the two iodinated materials are isostructural, consisting of columnar stacks of planar metallomacrocycles with parallel chains of disordered triiodide counterions, and that the two Ni(L) complexes have the same ionicity. The properties of both Ni(TBP)I and Ni(Pc)I are characteristic of "molecular metals", but the details of the charge-transport properties differ significantly and there are striking contrasts in the magnetic properties of the two materials. Thus, the two systems offer a unique opportunity to relate solid-state properties to the electronic structure of the parent complexes in the absence of any geometric or ionicity differences.

Probably the most unusual result of these comparisons concerns the nature of the charge carriers. The carriers in conducting molecular crystals have been found previously to belong to one of two limiting classes. Either they are confined to the d orbitals of a conducting metal spine as in the TCP salts, or they are associated with delocalized 2p $\pi$ molecular orbitals as in the organic conductors.[8,16] In our previous studies of molecular conductors formed by iodine oxidation of porphyrin-like Ni(L) complexes,[1-5] including Ni(Pc), we observed that electrons are removed from the ligand $\pi$ system and not from the metal. In these materials the metal retains its formal $Ni^{II}$ oxidation state and plays a secondary role in the conduction process, while the charge carriers are associated with delocalized $\pi$ orbitals on the macrocycle. However, we find Ni(TBP)I to be the first well-characterized, partially oxidized complex in which the charge carriers exhibit both metal and ligand properties. It appears that the electron hole created by iodine oxidation can jump between the metal and the macrocycle, as well as between one Ni(TBP) unit and its neighbors. In short, this complex displays a novel, doubly mixed valence state. There is a mixed valency along a Ni(TBP) stack, which may be made explicit by writing the stoichiometric formula as $[Ni(TBP)]_2[Ni(TBP)]^+(I_3^-)$. In addition, there is a second form of mixed valency within an individual oxidized complex; the $[Ni(TBP)]^+$ cation itself exhibits an interconversion between the electronic tautomers, $[Ni^{II}(TBP)^+]$ and $[Ni^{III}(TBP)]$. Thus, this compound shows characteristics intermediate between those of the metal-spine conductors and the organic conductors.

## Experimental Section

**Syntheses.** Zn(TBP) was synthesized by the template cyclization of isoindoline-3-acetic acid[17] with zinc acetate dihydrate using the method of Edwards, Gouterman, and Rose,[18] except that the samples were heated at 240 °C for 4 h under a slight positive pressure of nitrogen. An alternative synthesis, involving the template cyclization of acetophenone-2-carboxylic acid and zinc acetate, was also employed.[19] Metal-free TBP was obtained from the demetalation of Zn(TBP) by concentrated sulfuric acid.[18]

**(Tetrabenzoporphyrinato)nickel(II).** Ni(TBP) was prepared, apparently for the first time, from $H_2$(TBP) and nickel acetate in refluxing pyridine. To 120 mL of pyridine was added 400 mg (0.79 mmol) of $H_2$(TBP) and a large molar excess (2 g, 11.3 mmol) of $Ni(OAc)_2 \cdot 4H_2O$. The mixture was refluxed for 24 h and filtered hot. The pyridine solution was evaporated to dryness on a steam bath. The remaining solid was stirred in boiling $H_2O$, filtered, washed with acetone until the washings were colorless, and then dried. The procedure yielded 372 mg (0.66 mmol, 83%) of Ni(TBP). The material was purified by recrystallization from 1,2,4-trichlorobenzene. Anal. Calcd for $C_{36}H_{20}N_4Ni$: C, 76.22; H, 3.55; N, 9.87. Found: C, 76.35; H, 3.86; N, 9.52.

**Ni(TBP)$I_{1.0}$.** Solutions of Ni(TBP) in 1,2,4-trichlorobenzene were oxidized with elemental iodine by diffusion in an H-tube,[1c] and the small, shiny, dark green needles of Ni(TBP)I were collected by filtration. Anal. Calcd for $C_{36}H_{20}I_{1.0}N_4Ni$: C, 62.29; H, 2.90; N, 8.07. Found: C, 61.66; H, 2.99; N, 8.07.

**Resonance Raman Studies.** Ambient temperature resonance Raman measurements were made on microcrystalline samples contained in spinning (~1200 rpm) 5-mm Pyrex tubes,[1c,2b] using a spectrometer described elsewhere.[20] A number of scans were made at different laser powers to check for sample decomposition. The raw data were corrected for base line, background, and, where needed, plasma lines.

**Magnetic Measurements.** Electron paramagnetic resonance spectra at ca. 9 GHz were obtained on a modified Varian E-4 spectrometer. Frequencies of 12 GHz were obtained by interfacing a Varian klystron (Type V287M) and a 9-in. magnet (Varian No. 2500) to the spectrometer. The cavity resonance frequency was measured by a transfer oscillator technique to an accuracy of 5 ppm. The magnetic field was calibrated with DPPH ($g = 2.0036$) and Fremy's salt ($g = 2.0055$, $a^N = 13.0$ G). Temperature-dependent EPR measurements were obtained as previously reported.[2b] EPR powder spectrum simulations were calculated on a CDC 6600 computer using the program SIM14.[21] Experimental spectra taken at 12 GHz were sufficiently well resolved that the $g$ values corresponding to the individual $\mathbf{g}$ tensor axes ($g_\parallel$ and $g_\perp$) and the line widths ($\Gamma_\parallel$ and $\Gamma_\perp$) were obtained. In the 9-GHz spectra, however, the powder patterns were nearly symmetric and became increasingly so with cooling (see below). Computer simulations of these spectra show that the $g$ value calculated from the first derivative crossing point does not differ significantly from the average $g$ value, $g_{av} = (g_\parallel + 2g_\perp)/3$,[22] and similarly, that the derivative peak-to-peak line width, $\Gamma$, is a reasonable approximation to the average component line width.

EPR intensity measurements were obtained from numerical double integrations performed on a Fabritek Model 1074 instrument computer, using scan widths of at least 10 line widths. Absolute EPR intensities were calculated at room temperature by comparing the integrated absorption of the sample with that of a known amount of DPPH ($n = 0.89$ spins/molecule)[23a] dispersed in KBr. The static susceptibility, $\chi$, was measured by the Faraday technique as reported earlier[2b] using $Hg(Co(SCN)_4)$[23b] ($16.44 \times 10^{-6}$ cmu/g) as a standard.

**Electrical Conductivity Measurements.** Single-crystal conductivity measurements were made by using a four-probe ac phase locked technique. The crystals were mounted on thin carbon fibers by using integrated circuit cans prepared as previously described.[24] A graphite fiber

(14) (a) Miller, J. S.; Epstein, A. J. *J. Am. Chem. Soc.* **1978**, *100*, 1639–1641. (b) Torrance, J. B.; Mayerle, J. J.; Bechgaard, K.; Silverman, B. D.; Tomkiewicz, Y. *Phys. Rev. B* **1980**, *22*, 4960–4965. (c) Hawley, M. E.; Poehler, T. O.; Carruthers, T. F.; Bloch, A. N.; Cowan, D. O.; Kistenmacher, T. J. *Bull. Am. Phys. Soc.* **1978**, *23*, 424. (d) Stokes, J. P.; Bloch, A. N.; Bryden, W. A.; Cowan, D. O.; Hawley, M. E.; Poehler, T. O. *Ibid.* **1979**, *24*, 232. (e) Hawley, M. E.; Bryden, W. A.; Bloch, A. N.; Cowan, D. O.; Poehler, T. O.; Stokes, J. P. *Ibid.* **1979**, *24*, 232.

(15) As evidenced, for example, by the visible spectra. See: Solovev, K. N.; Mashenkov, V. A.; Kachura, T. F. *Opt. Spectrosc.* **1969**, *27*, 24–29.

(16) Kalina, D. W.; Lyding, J. W.; Ratajack, M. T.; Kannewurf, C. R.; Marks, T. J. *J. Am. Chem. Soc.* **1980**, *102*, 7854–7862 and references therein.

(17) Linstead, R. P.; Weiss, F. T. *J. Chem. Soc.* **1950**, 2975–2981.

(18) Edwards, L.; Gouterman, M.; Rose, C. B. *J. Am. Chem. Soc.* **1976**, *98*, 7638–7641.

(19) Vogler, A.; Kunkely, H. *Angew. Chem., Int. Ed. Engl.* **1978**, *17*, 760.

(20) Shriver, D. F.; Dunn, J. B. R. *Appl. Spectrosc.* **1974**, *28*, 319–323.

(21) Lozos, G. P.; Hoffman, B. M.; Franz, C. "SIM14", *QCPE* **1972**, *256*.

(22) Hyde, J. S.; Pilbrow, J. R. *J. Magn. Reson.*, in press.

(23) (a) Duffy, W., Jr.; Strandburg, D. L. *J. Chem. Phys.* **1967**, *46*, 456–464. (b) Figgis, B. N.; Nyholm, R. S. *J. Chem. Soc.* **1958**, 4190–4191.

(24) Phillips, T. E.; Anderson, J. R.; Schramm, C. J.; Hoffman, B. M. *Rev. Sci. Instrum.* **1979**, *50*, 263–265.

was attached to each of four 0.13-mm Al wires of the can by using a conducting palladium paint.[2b] These fibers were then attached to a crystal with the same conducting paint.

Measurements were normally taken at a frequency of 27 Hz and a sampling current of 10 μA; however, no differences were observed if the frequency was varied between 5 Hz and 2 kHz, and ohmic behavior was confirmed in a crystal current range of 1 μA to 10 mA. Contact integrity was verified by the lead interchange technique.[25]

The conductivity of the material was calculated from the relation $\sigma = L/RA$, where $\sigma$ is the conductivity in S cm$^{-1}$, $R$ is the measured resistance of the material between the two inner contacts in Ω, $L$ is the separation between the two inner contacts in cm, and $A$ is the cross-sectional area of the crystal in cm$^2$. Typically the crystals are 0.1 cm long and have a rectangular cross-section with the long width ~0.004 cm and the short width ~0.002 cm. The value of $L$ is usually around 0.02 cm. An empirical analysis of measurement errors[1c] indicates an uncertainty in the conductivity of $\delta\sigma/\sigma \approx \pm 0.2$.

**X-ray Study of Ni(TBP)$I_{1.0}$.** Ni(TBP)I was assigned to the Laue group $4/mmm$ on the basis of Weissenberg and precession X-ray photographs; these photographs are superimposable on those of Ni(Pc)I. Systematic absences were observed for reflections $0kl$ and $hhl$ with $l$ odd, consistent with the space groups $P4/mcc$ or $P4cc$. The successful refinement of the structure supports the choice of space group $D_{4h}^2$—$P4/mcc$. The cell constants of $a$ = 14.081 (25) Å and $c$ = 6.434 (11) Å at 113 K were found by a least-squares refinement[26] of 14 hand-centered reflections on a FACS-I diffractometer employing Mo Kα radiation. The Ni(TBP)I and Ni(Pc)I systems both crystallize in the same space group and display very similar X-ray photographs. Thus it seemed likely that the Ni(TBP)I and Ni(Pc)I systems were isostructural, and this was confirmed upon solution of the structure of Ni(TBP)I. In addition to the normal Bragg scattering, diffuse scattering was observed in Ni(TBP)I in oscillation and precession photographs in planes perpendicular to the $c^*$ axis. Diffuse scattering in similar systems,[27-29] most notably the Ni(Pc)I system,[1c] has been attributed to disorder along the iodine chain. The diffuse layers can be indexed on the basis of a superstructure spacing of 9.81 (8) Å at 300 K, which is typical of systems containing iodine in the form of triiodide ions.[1c,27,29]

Intensity data for the Bragg scattering were collected at 113 (3) K by the $\theta$–$2\theta$ scan technique and were processed[30] with the use of a value of 0.04 for $p$. No systematic change was detected in the intensities of six standard reflections which were measured every 100 reflections. A total of 954 unique reflections was gathered, 330 of which were found to have $F_o^2 > 3\sigma(F_o^2)$. No corrections for absorption or extinction were necessary. Experimental details and crystal data are given in Table I.

The positions of all nonhydrogen atoms relative to the nickel atom were found in an origin-removed, sharpened Patterson map. The asymmetric unit consists of one-eighth of the Ni(TBP) complex and one-eighth of an iodine atom. A site symmetry of $4/m$ or 422 is imposed crystallographically on the Ni species. From the chelate ring orientation obtained from the Patterson map, the site symmetry is $4/m$.

Initial full-matrix, least-squares refinements on $F_o$ using isotropic thermal parameters led to values for $R$ and $R_w$ of 0.131 and 0.136, respectively. When anisotropic thermal parameters were used for the Ni and I atoms, $R$ and $R_w$ decreased to 0.064 and 0.076. All hydrogen positions were located from a difference Fourier map. Their positions were idealized (C–H = 0.95 Å) and were not varied through the remainder of the refinement. Each hydrogen atom was given a thermal parameter of 1 Å$^2$ greater than that of the carbon atom to which it is bonded. The final refinement on $F_o^2$ with variable anisotropic thermal parameters for all nonhydrogen atoms led to values for $R$ and $R_w$ on $F_o^2$ of 0.122 and 0.164, respectively. In this cycle of refinement, there were 65 variables and 954 observations (including $F_o^2 \leq 0$). An analysis of $\sum w(F_o^2 - F_c^2)^2$, with $w = 1/\sigma^2(F_o^2)$, as a function of $F_o^2$, scattering angles, and Miller indices shows no unusual trends. The highest peak in the final difference electron density map (3.1 e/Å$^3$) is located near the iodine; the map has no other outstanding features.

The final positional and thermal parameters are given in Table II. Root-mean-square amplitudes of vibration are given in Table III.[31] A listing of the observed and calculated structure amplitudes is also available.[31] In this listing an entry with $F_o$ negative symbolizes a reflection having $F_o^2 < 0$.

Table I. Crystal Data and Experimental Details for Ni(TBP)I

| | |
|---|---|
| compd | (tetrabenzoporphyrinato)nickel(II) iodide |
| formula | $C_{36}H_{20}IN_4Ni$ |
| Fw, amu | 694.20 |
| cell | |
| $a$, Å | 14.081 (25) |
| $c$, Å | 6.434 (11) |
| $V$, Å$^3$ | 1276 |
| $Z$ | 2 |
| $d$(calcd), g/cm$^3$ | 1.806 (113 K) |
| $d$(obsd),[a] g/cm$^3$ | 1.72 (2) (298 K) |
| space group | $D_{4h}^2$–$P4/mcc$ |
| cryst shape | needle of square cross-section bounded by faces of the forms {100} and {001} with separations of 0.036 and 0.334 mm, respectively |
| cryst vol, mm$^3$ | 0.00043 |
| radiatn | graphite-monochromated Mo Kα ($\lambda$(Mo K$\alpha_1$) = 0.7093 Å) |
| $\mu$, cm$^{-1}$ | 20.0 |
| transmissn factors | 0.928–0.935 |
| takeoff angle, deg | 2.5 |
| receiving aperture | 6.0 mm high × 6.0 mm wide; 34 cm from crystal |
| scan speed, deg/min | 2 |
| scan width, deg | 0.80 below K$\alpha_1$ to 0.80 above K$\alpha_2$ |
| bkgd counts | 20 s with rescan option $4° \leq 2\theta \leq 50°$, $l \geq 0$; 40 s, $50° \leq 2\theta \leq 58.4°$, $l \geq 0$; $4° \leq 2\theta \leq 58.4°$, $l < 0$ |
| data collected | $h \geq k \geq 0$; $\pm l$, $4° \leq 2\theta \leq 58.4°$ |
| unique data after averaging | 954 |
| unique data with $F_o^2 > 0$ | 766 |
| unique data with $F_o^2 \geq 3\sigma(F_o^2)$ | 330 |
| no. of variables | 65 |
| $R$ on $F_o^2$ | 0.122 |
| $R_w$ on $F_o^2$ | 0.164 |
| $R$ on $F_o$, $F_o^2 > 3\sigma(F_o^2)$ | 0.055 |
| $R_w$ on $F_o$, $F_o^2 > 3\sigma(F_o^2)$ | 0.063 |

[a] Flotation in $ZnCl_2/H_2O$.

## Results

**Resonance Raman Spectra.** Determination of the form of the iodine species is important in relating the transport properties of Ni(TBP)I to the degree of oxidation or ionicity of the macrocycle. The ionicity cannot be obtained from the stoichiometric formula alone, since the charge on the macrocyclic complex is determined by the form of the iodine ($I_2$, $I^-$, $I_3^-$, $I_5^-$, etc.) in the crystal. One useful method for the determination of the form of the iodine is resonance Raman spectroscopy.[32] The resonance Raman spectrum of Ni(TBP)I shows a sharp absorption at 107 cm$^{-1}$, with an overtone progression at 217, 328, and 432 cm$^{-1}$. These wavelengths are characteristic of chains of symmetrical $I_3^-$ ions. The absence of any sharp peaks at 212 and 167 cm$^{-1}$ precludes sizable amounts (>2%) of $I_2$ and $I_5^-$, respectively. Since $^{129}I$

(25) Schafer, D. E.; Wudl, F.; Thomas, G. A.; Ferraris, J. P.; Cowan, D. O. *Solid State Commun.* **1974**, *14*, 347–351.
(26) Corfield, P. W. R.; Doedens, R. J.; Ibers, J. A. *Inorg. Chem.* **1967**, *6*, 197–204.
(27) Endres, H.; Keller, H. J.; Megnamisi-Belombe, M.; Moroni, W.; Pritzkow, H.; Weiss, J.; Comeš, R. *Acta Crystallogr., Sect. A* **1976**, *A32*, 954–957.
(28) Cowie, M.; Gleizes, A.; Grynkewich, G. W.; Kalina, D. W.; McClure, M. S.; Scaringe, R. P.; Teitelbaum, R. C.; Ruby, S. L.; Ibers, J. A.; Kannewurf, C. R.; Marks, T. J. *J. Am. Chem. Soc.* **1979**, *101*, 2921–2936.
(29) Smith, D. L.; Luss, H. R. *Acta Crystallogr., Sect. B* **1977**, *B33*, 1744–1749.
(30) The Northwestern absorption program, AGNOST, includes both the Coppens–Leiserowitz–Rabinovich logic for Gaussian integration and the Tompa analytical method. In addition to various local programs for the CDC 6600 computer, modified versions of the following programs were employed: Zalkin's FORDAP Fourier summation program, Johnson's ORTEP thermal ellipsoid plotting program, and Busing's and Levy's ORFFE error function program. Our full-matrix, least-squares program, NUCLS, in its nongroup form, closely resembles the Busing–Levy ORFLS program. The diffractometer was run under the disk-oriented Vanderbilt system (Lenhert, P. G. *J. App. Crystallogr.* **1975**, *8*, 568–570).
(31) Supplementary material.
(32) (a) Teitelbaum, R. C.; Ruby, S. L.; Marks, T. J. *J. Am. Chem. Soc.* **1978**, *100*, 3215–3217. (b) Teitelbaum, R. C.; Ruby, S. L.; Marks, T. J. *Ibid.* **1980**, *102*, 3322–3328.

Table II. Positional and Thermal Parameters for the Atoms of Ni(TBP)I

| ATOM | X[A] | Y | Z | B11[B] OR B,A[2] | B22 | B33 | B12 | B13 | B23 |
|---|---|---|---|---|---|---|---|---|---|
| I | 1/2 | 1/2 | 1/4 | 31.23(65) | 31.23 | 417.1(66) | 0 | 0 | 0 |
| NI | 0 | 0 | 0 | 16.79(80) | 16.79 | 92.0(53) | 0 | 0 | 0 |
| N | 0.05819(61) | 0.12687(58) | 0 | 16.0(45) | 17.9(46) | 93.(19) | -5.6(38) | 0 | 0 |
| C(1) | 0.15550(84) | 0.14756(73) | 0 | 32.2(71) | 2.9(51) | 65.(16) | -5.4(38) | 0 | 0 |
| C(2) | 0.17123(69) | 0.24884(81) | 0 | 22.3(57) | 20.8(55) | 107.(24) | 2.1(47) | 0 | 0 |
| C(3) | 0.25233(81) | 0.30533(76) | 0 | 24.4(59) | 27.1(57) | 101.(23) | -7.5(51) | 0 | 0 |
| C(4) | 0.24204(92) | 0.40316(79) | 0 | 36.5(72) | 23.0(61) | 203.(34) | -5.5(58) | 0 | 0 |
| C(5) | 0.15199(92) | 0.44375(73) | 0 | 38.9(73) | 6.7(51) | 301.(40) | -5.5(49) | 0 | 0 |
| C(6) | 0.06960(81) | 0.38873(82) | 0 | 30.5(68) | 22.8(68) | 166.(29) | 3.9(52) | 0 | 0 |
| C(7) | 0.08215(79) | 0.29143(77) | 0 | 28.9(67) | 17.2(58) | 115.(25) | -1.6(50) | 0 | 0 |
| C(8) | 0.01209(99) | 0.21337(72) | 0 | 43.7(87) | 24.2(55) | 57.(17) | 8.3(54) | 0 | 0 |
| C(9) | 0.22605(78) | 0.08370(73) | 0 | 26.7(63) | 17.3(55) | 66.(22) | 0.4(48) | 0 | 0 |
| H1C(3) | 0.316 | 0.278 | 0 | 3.0 | | | | | |
| H1C(4) | 0.299 | 0.443 | 0 | 3.4 | | | | | |
| H1C(5) | 0.148 | 0.513 | 0 | 3.8 | | | | | |
| H1C(6) | 0.005 | 0.415 | 0 | 3.0 | | | | | |
| H1C(9) | 0.292 | 0.107 | 0 | 2.3 | | | | | |

[a] Estimated standard deviations in the least significant figure(s) are given in parentheses in this and all subsequent tables. [b] The form of the anisotropic thermal ellipsoid is $\exp[-(B_{11}h^2 + B_{22}k^2 + B_{33}l^2 + 2B_{12}hk + 2B_{13}hl + 2B_{23}kl)]$. The quantities given in the table are the thermal coefficients $\times 10^4$.

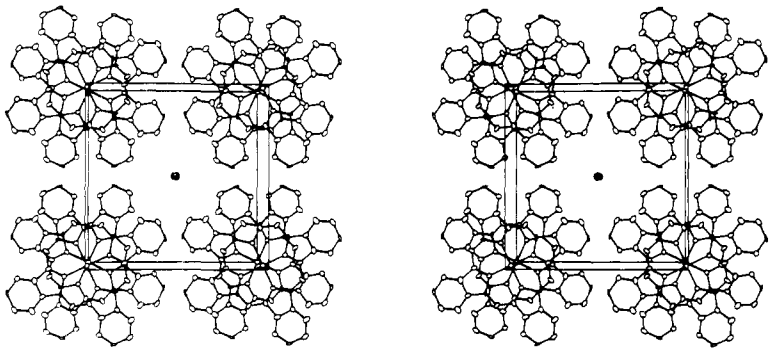

Figure 1. Stereoview of the crystal packing in Ni(TBP)I. Hydrogen atoms are not shown.

Mössbauer spectroscopy of the related complex Ni(Pc)I (vide infra) indicates a complete absence of $I^-$,[1a,c] we assume this is also true for Ni(TBP)I. As a result, a reasonable formulation of $Ni(TBP)I_{1.0}$ is $[Ni(TBP)]^{\rho+}(I_3^-)$, where $\rho = 0.33$ is the actual degree of partial oxidation of the macrocycle.

**Description of the Structure.** As we anticipated from the similarities in the space group, unit cell constants, and X-ray photographs of the Ni(TBP)I and Ni(Pc)I systems, all major features of the two structures are identical. The crystal packing in Ni(TBP)I is the same as that in Ni(Pc)I[1c] consisting of metallomacrocycle stacks that are segregated from linear chains of iodine, both of which run parallel to the $z$ axis. The iodine chains lie in channels formed by the benzo groups of neighboring Ni(TBP) molecules, as can be seen in the stereoview of the crystal packing shown in Figure 1. Successive Ni(TBP) molecules in a stack are staggered by 41°. Each Ni(TBP) molecule is on a site of $4/m$ symmetry and consequently is constrained to be planar with the normal to the plane parallel to the stacking axis. The resultant metal-over-metal stacking is a feature which has been present in all of the iodine-oxidized metallomacrocyclic systems.[1c,2b,28,33,34] The iodine atoms are on sites of 422 symmetry. The thermal parameter for iodine along the chain direction is more than twice that perpendicular to the chain. This has been observed previously[1c,27,34] and is attributed to ordered chains of $I_3^-$ ions which are disordered with respect to their neighbors. It is this disorder which gives rise to the observed diffuse intensity. The diffuse planes are normal to the $c$ axis and, as was true for Ni(Pc)I, the superstructure spacing ($c'$) corresponds to $^3/_2c$. Since $c'$ is a multiple of $c$, the iodine superlattice is commensurate with the Bragg lattice with a repeat unit which contains three Bragg sites. A detailed analysis of the diffuse X-ray scattering, which was carried out for Ni(Pc)I,[1c] was not attempted for Ni(TBP)I. However, since the Ni(Pc)I and Ni(TBP)I crystals have isostructural macrocycle stacks and contain identical amounts of iodine in triiodide chains with equivalent superlattice spacings, we believe that the model of disorder for the triiodide chains in Ni(Pc)I is applicable to Ni(TBP)I as well.

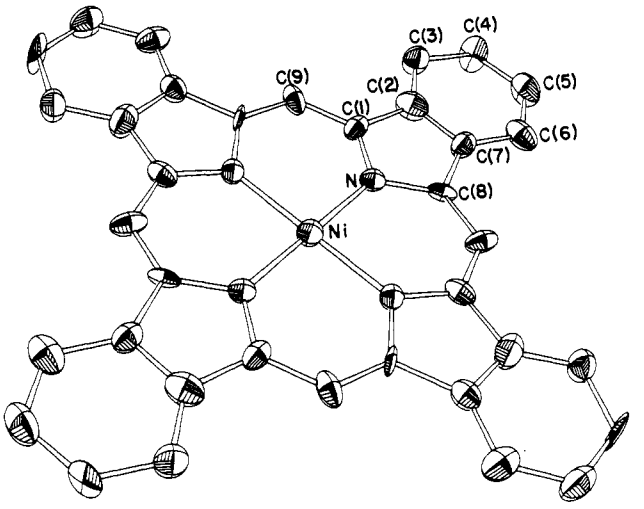


Figure 2. Perspective view of the Ni(TBP) molecule, hydrogen atoms omitted.

A perspective drawing of the Ni(TBP) molecule is shown in Figure 2. Bond distances and angles are given in Table IV. As

(33) (a) Endres, H.; Keller, H. J.; Moroni, W.; Weiss, J. *Acta Crystallogr., Sect. B* **1975**, *B31*, 2357–2358. (b) Brown, L. D.; Kalina, D. W.; McClure, M. S.; Schultz, S.; Ruby, S. L.; Ibers, J. A.; Kannewurf, C. R.; Marks, T. J. *J. Am. Chem. Soc.* **1979**, *101*, 2937–2947.

(34) Gleizes, A.; Marks, T. J.; Ibers, J. A. *J. Am. Chem. Soc.* **1975**, *97*, 3545–3546.

Table IV. Observed Distances and Angles in Ni(TBP)I

| | Distances, Å | | |
|---|---|---|---|
| Ni-N | 1.966 (9) | C(2)-C(7) | 1.391 (15) |
| N-C(1) | 1.401 (13) | C(3)-C(4) | 1.385 (15) |
| N-C(8) | 1.380 (13) | C(4)-C(5) | 1.391 (17) |
| C(9)-C(1) | 1.340 (15) | C(5)-C(6) | 1.395 (16) |
| C(9)-C(8') | 1.361 (16) | C(6)-C(7) | 1.382 (15) |
| C(1)-C(2) | 1.443 (14) | C(7)-C(8) | 1.477 (15) |
| C(2)-C(3) | 1.392 (14) | | |
| | Angles, Deg | | |
| N-Ni-N' | 90.00 | C(2)-C(3)-C(4) | 118.9 (12) |
| Ni-N-C(1) | 126.6 (7) | C(3)-C(4)-C(5) | 120.3 (11) |
| Ni-N-C(8) | 127.3 (8) | C(4)-C(5)-C(6) | 122.0 (10) |
| C(1)-N-C(8) | 106.1 (9) | C(5)-C(6)-C(7) | 116.4 (11) |
| C(1)-C(9)-C(8') | 124.6 (11) | C(2)-C(7)-C(6) | 122.9 (11) |
| C(9)-C(1)-N | 125.8 (9) | C(2)-C(7)-C(8) | 106.4 (10) |
| C(9)-C(1)-C(2) | 123.3 (10) | C(6)-C(7)-C(8) | 130.8 (11) |
| N-C(1)-C(2) | 110.8 (10) | C(9)-C(8)-N | 125.6 (11) |
| C(3)-C(2)-C(7) | 119.6 (10) | C(9)-C(8)-C(7) | 124.4 (10) |
| C(1)-C(2)-C(3) | 133.7 (10) | N-C(8)-C(7) | 110.0 (11) |
| C(1)-C(2)-C(7) | 106.7 (10) | | |

is true for the crystal packing, the molecular structure of Ni(TBP)I is also very similar to that of Ni(Pc)I.[1c] One of the major differences between the two structures is the larger Ni–N bond distance in Ni(TBP)I (1.966 (9) Å vs. 1.887 (6) Å for Ni(Pc)I). This reflects the larger central hole present in a tetrabenzoporphyrin ring as compared with a phthalocyanine ring. A similar Ni–N bond distance (1.953 (5) Å) was found for Ni(OMTBP)$I_{1.08}$,[2b] the only other reported structure of a metallotetrabenzoporphyrin. The C(1)–C(9)–C(8) angle of the methine bridge in Ni(TBP)I (124.6 (11)°) is identical with that of Ni(OMTBP)I (124.7 (7)°) but is larger than the corresponding C(1)–N–C(8) angle of the azomethine bridge in Ni(Pc)I (119.2 (6)°). The angle contraction in Ni(Pc)I probably arises from the steric effects of the lone-pair electrons on the nitrogen atom.[35]

The closest intermolecular contacts in the Ni(TBP) stack are C(1)–C(1′) and C(8)–C(8′) at 3.221 (5) and 3.235 (6) Å, respectively. These may be compared with values of 3.252 (2) and 3.258 (2) Å for the same interactions in Ni(Pc)I. The *c* spacing increases in Ni(TBP)I from 6.434 (11) Å at 113 K to 6.53 (3) Å, as obtained from film data at 300 K. This corresponds to an increase of the Ni–Ni separation from 3.217 (5) to 3.26 (2) Å, or slightly over 1%. The Ni–Ni separation for Ni(TBP)I at 300 K is very close to that of 3.244 (2) Å found for Ni(Pc)I at the same temperature.

**Magnetic Measurements.** Oxidation of a metalloporphyrin can proceed by oxidation of the macrocycle to create a $\pi$-cation radical with one of two symmetries ($A_{1u}$, $A_{2u}$)[36] or by oxidation of the central metal ion. EPR and static susceptibility measurements of Ni(TBP)I have been used to characterize both the hole species created upon formation of the mixed valency solid and the intermolecular interactions which occur within a partially oxidized Ni(TBP) stack.

**Magnetic Measurements. Observations.** The room-temperature EPR spectra obtained from polycrystalline samples of Ni(TBP)I show a roughly symmetric line with an isotropic *g* value, $g_{av}$ = 2.024, which is unusually large in comparison with those of other M(L)$I_x$ systems (Table V), and with a large peak-to-peak line width, $\Gamma$ = 105 G. It is because of this large line width that single-crystal resonances are not observable. A closer examination of the signal reveals it to be slightly asymmetric, with a broadening to low field. At a higher frequency, 11.96 GHz, the broadening is pronounced and the spectrum can be satisfactorily computer-simulated by using a Lorentzian component line shape with $g_\parallel$ = 2.060 (5) and $g_\perp$ = 2.018 (5) and with the principal peak-to-peak line width values of $\Gamma_\parallel$ = 110 (6) G and $\Gamma_\perp$ = 75 (5) G

Table V. Room-Temperature EPR *g* Values and Line Widths for Ni(L)$I_x$ Systems

| | $g_\parallel$ | $g_\perp$ | $\Gamma_\parallel$, G | $\Gamma_\perp$, G |
|---|---|---|---|---|
| Ni(TBP)I[a] | 2.060 | 2.018 | 110 | 75 |
| Ni(OMTBP)$I_{1.08}$[b] | 2.0102 | 2.0033 | 5.23 | 3.51 |
| Ni(Pc)$I_{1.0}$[c] | 2.0075 | 2.0007 | 5.32 | 3.56 |
| Ni(OEP)$I_{1.2}$[d,e] | 2.0072[f] | | 17.10[f] | |

[a] The alternative fit yields $g_\parallel$ = 2.00, $g_\perp$ = 2.03, $\Gamma_\parallel$ = 50 G, and $\Gamma_\perp$ = 95 G. [b] Reference 2b. [c] Reference 1c. [d] OEP = 1,2,3,4,5,6,7,8-octaethylporphyrinato.[4] [e] Iodine in $I_5^-$ form. [f] Component values not resolved.

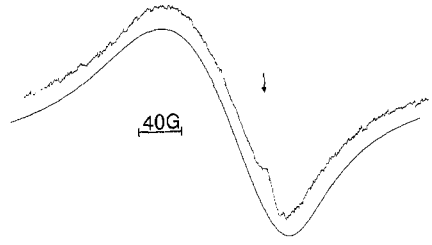


**Figure 3.** Room-temperature 11.96-GHz powder EPR spectrum for Ni(TBP)I: experimental (upper); simulation (lower), based on the parameters $g_\parallel$ = 2.060, $g_\perp$ = 2.018, $\Gamma_\parallel$ = 110 G, and $\Gamma_\perp$ = 75 G. This simulation is virtually indistinguishable from that based on the parameters $g_\parallel$ = 2.00, $g_\perp$ = 2.03, $\Gamma_\parallel$ = 50 G, and $\Gamma_\perp$ = 95 G. Arrow indicates position of DPPH resonance. A small *g* = 2.0006 impurity signal is visible on the high-field half of the signal.

(Figure 3). The trend of $g_\parallel > g_\perp$ is consistent with previous studies;[1,2] however, the fit is not unique, with an equally good alternative set of parameters being $g_\parallel$ = 2.00, $g_\perp$ = 2.03, $\Gamma_\parallel$ = 50 G, and $\Gamma_\perp$ = 95 G. Quantitation of the intensity of the room-temperature signal from many different samples shows that it corresponds to an invariant number of $S = {}^1/_2$ spins/g, and so we assign it as the intrinsic EPR signal associated with the partially oxidized, conducting state.

Depending on the exact procedure used for the oxidation and the particular sample, we frequently observe a weaker second signal with intensities ranging from less than $10^{-3}$ to almost 0.02 spins/macrocycle. This signal can be analyzed in terms of an axial **g** tensor with $g_\perp$ = 2.29. The feature associated with $g_\parallel$ blends into the intrinsic EPR signal, and so $g_\parallel$ can be only roughly estimated to have a value of ca. 2.1. On the basis of its variable intensity, this signal is considered to arise from an impurity.[37] In addition, at *g* = 2.0026, an isotropic and very sharp ($\Gamma$ = 4 G) impurity signal is sometimes found. It is very weak, with a room-temperature intensity of less than $4 \times 10^{-4}$ spins/macrocycle.

The room temperature spin susceptibility of polycrystalline Ni(TBP)I samples was measured by both EPR and static methods. The intrinsic EPR signal was numerically doubly integrated, and its area was compared with that from a known amount of DPPH. Depending on the sample, either the *g* = 2.0026 impurity signal was insignificant or its contribution was readily evident in the integrations and could be subtracted. The results were independent of sample and yielded a value of 0.09 (2) $S = {}^1/_2$ spins/macrocycle. The room-temperature static susceptibility was also measured, using a sample shown by EPR to contain a negligible impurity signal. The observed value, $\chi_m = -2.69 \times 10^{-4}$ emu/mol, was corrected for the temperature-independent diamagnetic susceptibility ($\chi^d = -3.59 \times 10^{-4}$ emu/mol for Ni(TBP)$I_{1.0}$, obtained from Pascal's constants[38]) to yield the paramagnetic susceptibility

(35) Hoard, J. L. In "Porphyrins and Metalloporphyrins", Smith, K. M., Ed.; American Elsevier: New York, 1975; pp 321–327.
(36) Gouterman, M.; Wagniere, G. H.; Snyder, L. C. *J. Mol. Spectrosc.* **1963**, *11*, 108–127.

(37) The **g** tensor of the large impurity signal corresponds to that expected for a material containing a metal-oxidized metallomacrocycle [$Ni^{III}$(L)]. In the synthesis of Zn(TBP), Vogler and Kunkely[19] report an impurity with a spectrum similar to pure Zn(TBP) but with an additional absorption at 460 nm. This impurity is not totally removed by either recrystallization or chromatographic techniques and is thus carried on through the synthesis of Ni(TBP). It is reasonable to propose that this impurity is structurally related to Ni(TBP), and that upon $I_2$ oxidation, it forms a $Ni^{III}$ species which then cocrystallizes to a variable extent with the authentic Ni(TBP) species.

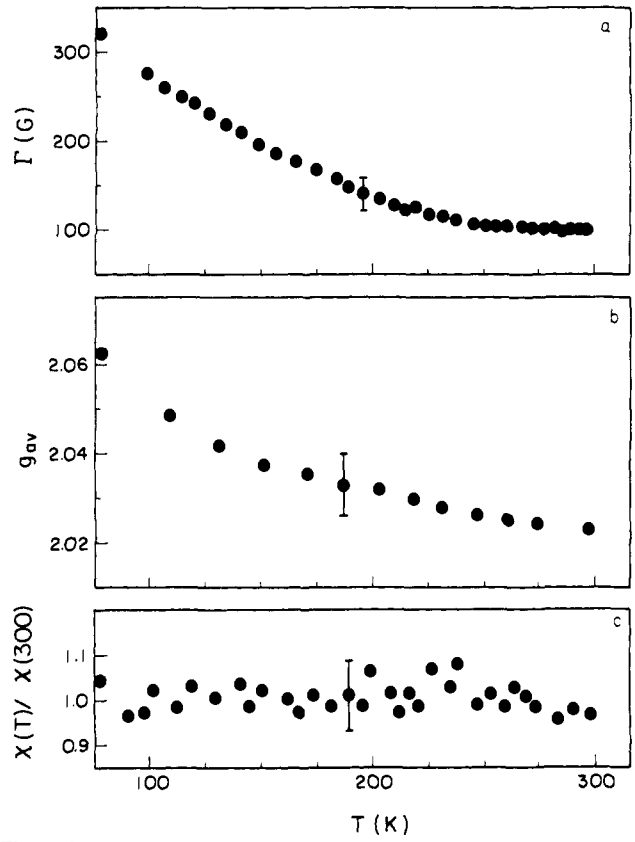


**Figure 4.** Temperature dependence of (a) EPR powder line width, (b) $g_{av}$ value, and (c) relative spin susceptibility of Ni(TBP)I.

of $\chi^p = 9\ (1) \times 10^{-5}$ emu/mol. Assuming a spin-only formalism and the values $S = {}^1/_2$ and $g = 2$, we calculate 0.07 (4) spins/macrocycle, in agreement with the value obtained from integrated EPR intensity.

The temperature variation of the Ni(TBP)I intrinsic spin susceptibility was obtained by measuring the EPR intensity from 77 to 300 K (Figure 4c). The susceptibility is constant over this range and thus has the appearance of the Pauli paramagnetism of a degenerate electron gas. The two impurity signals were also examined and were found to increase in intensity with decreasing temperature. The intrinsic spin susceptibility could not be quantified accurately for $T < 77$ K because of increasing interference from the Curie-like impurity signals; this problem was exacerbated by a temperature-dependent change in the resonance parameters as described immediately below. The static susceptibility measurements support the EPR result that $\chi_p$ is temperature independent down to at least 77 K.

Contrary to previous results for the conducting M(L)I systems,[1-5,7] including Ni(Pc)I, the $g$ values for the Ni(TBP)I intrinsic signal are strongly temperature dependent. The temperature dependence of $g_{av}$ was accurately measured by using the sharp impurity signal, which has a temperature-invariant isotropic $g$ value of 2.0026, as an internal standard. As the temperature is lowered, $g_{av}$ increases from 2.024 at 295 K to 2.062 at 77 K (Figure 4b). In the same temperature range, the signal broadens and becomes more symmetric; $\Gamma$ increases from 105 to 320 G (Figure 4a) and the slight asymmetry decreases, disappearing by 150 K. Spectra taken between 77 and 30 K show that $g_{av}$ and $\Gamma$ continue to increase, but accurate values could not be obtained because the intrinsic signal merges with the Curie-like $g = 2.29$ impurity signal. Below 30 K, even qualitative assessments as to the value of $g_{av}$ are not reliable; however, the line width appears to continue to increase.

**Magnetic Measurements. Analyses.** In our previous EPR studies of partially oxidized M(L)I systems, the observed g tensors were free radical like and characterized by the inequality $g_\parallel > g_\perp \approx g_e$, and they were analyzed in terms of a ligand-centered oxidation.[1-5,7] The deviation of $g_\parallel$ from $g_e$ was shown to be caused by a small spin density (<0.5%) on the iodine, arising from back charge transfer from $I_3^-$ to the macrocycle stack. As we now show, this explanation cannot account for the large deviations of both $g_\parallel$ and $g_\perp$ from $g_e$. The alternative explanation of a simple metal-centered oxidation of Ni(TBP) is also unacceptable, since it erroneously predicts a g tensor corresponding closely to the values of $g_\perp = 2.29 > g_\parallel = 2.11$ found for related $Ni^{III}$ macrocycles such as $[Ni^{III}(Pc)]$.[39] Instead, the g tensor for Ni(TBP)I reflects a hole state which is not purely ligand centered but contains appreciable metal-centered ($Ni^{III}(L)$) character, as well as the previously observed small contribution from iodine. In other words, not only are the Ni(TBP) macrocycles of Ni(TBP)I partially oxidized to a mixed valence state having an ionicity, or average charge, of $\rho = +1/3$ but also the individual cations themselves exhibit a mixed valency, with partial oxidation from the metal and from the macrocycle.

Consider a partially oxidized metallomacrocycle $M(L)^{\rho+}(I_3)_\rho$ in which the hole state is a combination of the planar $Ni^{III}$ and $\pi$-cation radical species. We have shown previously that the wave function for the $\pi$-cation radical may be written to include back charge transfer from the $I_3^-$ to macrocyclic stack, as shown in eq 1, where $\alpha^2$ is a measure of the degree of charge back-transferred

$$|\pi\rangle = (1 - \alpha^2)^{1/2}|[M^{II}(L)^{+\cdot}]_{\rho-1}(I_3^-)\rangle + \alpha|[M^{II}(L)]_{\rho-1}(I_3^{\cdot})\rangle \quad (1)$$

from the triiodide ion. Addition to this wave function of a term representing the contribution from a metal-oxidized $Ni^{III}$ species gives the phenomenological wave function

$$|\psi\rangle = \gamma|[M^{II}(L)^{+\cdot}]_{\rho-1}(I_3^-)\rangle + \beta|[M^{III}(L)]_{\rho-1}(I_3^-)\rangle + \alpha|[M(L)]_{\rho-1}(I_3^{\cdot})\rangle \quad (2)$$

If we ignore, for the moment, the small contribution from iodine, this equation describes a state in which the carriers have both $\pi$ and d character. The $g$ values for an $M(L)I_x$ compound described by eq 2 are found to be

$$g_i = \gamma^2 g_i(M^{II}(L)^{+\cdot}) + \beta^2 g_i(M^{III}(L)) + \alpha^2 g_i(I_3^{\cdot}) \quad (3)$$

where the normalization condition is $\gamma^2 + \beta^2 + \alpha^2 = 1$, $g_i$ represents either $g_\parallel$ or $g_\perp$, and reference $g$ values for the isolated component species are to be used. As discussed previously[1c,40] for a linear $I_3^{\cdot}$ radical in an axially symmetric field, the reference $g$ values are $g_\parallel(I_3^{\cdot}) = 4$ and $g_\perp(I_3^{\cdot}) = 0$. The reference g tensor for the $\pi$-cation radical configuration is taken to be isotropic, with value $g_e$, and for the $Ni^{III}$ configuration we employ $g_\parallel = 2.11$ and $g_\perp = 2.29$, as for $[Ni^{III}(Pc)]$.[39a] Equation 3 can then be solved to yield

$$\beta^2 = 2.53g_\parallel + 2.52g_\perp - 10.13 \quad (4)$$

$$\alpha^2 = 0.364g_\parallel - 0.136g_\perp - 0.456 \quad (5)$$

From the first set of room temperature Ni(TBP)I $g$ values given above, one obtains a metal d contribution of roughly ${}^1/_6$ ($\beta^2 = 0.16$), a ligand $\pi$ contribution of $\gamma^2 = 0.82$, and back charge transfer of $\alpha^2 = 0.02$. The second set of $g$ values still gives a large d contribution ($\beta^2 = 0.07$) but reduces the iodine contribution almost to zero.[41]

The observed temperature dependence of $g_{av}$ requires that the phenomenological coefficients in eq 2 be temperature dependent. The increase in the value of $g_{av}$ as the temperature is reduced (Figure 4b) indicates (eq 3) that the carrier spins become more d-like at low temperature. A quantitative treatment is hampered because poor spectral resolution precludes precise individual measurements of $g_\parallel$ and $g_\perp$ at low temperature. However, previous

(38) Weissenberger, A.; Rossiter, B. W. "Physical Methods of Chemistry"; Wiley-Interscience: New York, 1969; Vol. I, p 431.

(39) (a) Bobrovskii, A. P.; Sidorov, A. N. *J. Struct. Chem.* (*Engl. Transl.*) **1976**, *17*, 50–54. (b) Wolberg, A.; Manassen, J. *Inorg. Chem.* **1970**, *9*, 2365–2367.

(40) Atkins, P.; Symons, M. "The Structure of Inorganic Radicals"; Elsevier: Amsterdam, 1967.

(41) Euler, W. B.; Hoffman, B. M., manuscript in preparation.

studies on Ni(Pc)I[1c] and Ni(OMTBP)$I_{1.08}$[2b] show that the degree of back charge transfer ($\alpha^2/\gamma^2$) is temperature invariant, and this result is consistent with an analysis of $g_{av}(T)$ for Ni(TBP)I through use of eq 3–5. Upon introducing this constraint into eq 3, one finds that the low-temperature behavior of $g_{av}$ for Ni(TBP)I can indeed be explained by a large increase in the metal d contribution, which rises to almost $^1/_3$ by 77 K if one employs the first $g$ values analysis or to over $^1/_4$ if one employs the alternative analysis.

The value of 0.08 spins/macrocycle from the magnetic susceptibility is less than the value of 0.33 expected from the ionicity. A low and nearly temperature-independent value of $\chi$ is indicative of interactions among species on a conductive ML stack. One measure of intrastack, intermolecular interaction is obtained by considering a single tight-binding band composed of the highest occupied molecular orbitals on Ni(TBP).[8c] Upon partial oxidation by $\rho = {}^1/_3$, the Pauli susceptibility is given by eq 6,[1c,8c,42] where

$$\chi^s = Ng_\parallel{}^2\beta^2/[8\pi t \sin(5\pi/6)] \quad (6)$$

$N$ is Avogadro's number, $\beta$ is the Bohr magneton, and $t$ is the transfer integral (a direct analogue of the Huckel $\beta$). Using our value of $9.0 \times 10^{-5}$ emu/mol for $\chi^s$, we obtain a value for the transfer integral of 0.11 eV, or a bandwidth of $4t = 0.44$ eV. This is essentially identical with the value of 0.37 eV similarly determined for Ni(Pc)I[1c] and compares favorably with the 0.2–0.7-eV range determined by various experiments for the bandwidth of the organic conductor TTF–TCNQ.[43] A more detailed treatment which considers contributions both from metal- and ligand-localized electrons will be presented elsewhere.[41]

The line width of the Ni(TBP)I EPR spectrum is strikingly different from that of the isostructural compound Ni(Pc)I. First, the room-temperature line widths of Ni(TBP)I ($\Gamma_\parallel$ = 110 G and $\Gamma_\perp$ = 75 G) are ca. 20 times larger than those of Ni(Pc)I ($\Gamma_\parallel$ = 5.3 G and $\Gamma_\perp$ = 3.8 G). Second, the Ni(TBP)I line width increases markedly at lower temperatures while that of Ni(Pc)I decreases slightly. Analysis of the $g$ values for the two compounds shows an unusual characteristic of the Ni(TBP)I carrier spins, namely, the large d character. In addition, it is possible that the iodine character is as much as 10 times greater for Ni(TBP)I than for Ni(Pc)I.[1c] Our analysis of the line width of Ni(OMTBP)$I_{1.08}$ disclosed a contribution to the line width from spin density on iodine.[3] Therefore some of the room-temperature breadth of the Ni(TBP)I line could be associated with spin density on iodine. However, in other highly conducting systems whose broad room-temperature EPR lines ($\Gamma > 100$ G) are attributed to spin–orbit coupling on iodine, the line width decreases as the temperature is lowered,[12b,44] in contrast to the present observations. Instead, it is clear that the unusual temperature dependence of the Ni(TBP)I line width is primarily associated with the d electron character of the spins. This may be seen by noting the similarity in the temperature dependences of $\Gamma(T)$ and $g_{av}(T)$ (Figure 4). Since the temperature dependence of $g(T)$ is interpreted as reflecting changes in d character, this observation indicates that the unusual characteristics of the Ni(TBP)I EPR line width are also a consequence of the large d contribution to the carrier spins.

**Conductivity.** The room-temperature, single-crystal conductivity along the stacking axis, $\sigma_\parallel{}^{RT}$, has been measured for more than 20 samples of Ni(TBP)I. Depending on the quality of the crystal, we find values from 150 to 330 S cm$^{-1}$, a range which overlaps that observed for single crystals of the isostructural compound, Ni(Pc)I (250–750 S cm$^{-1}$),[1c] and which is comparable with values reported for other one-dimensional metals such as the TCP salts and the organic TCNQ salts.[8] The temperature dependence of single-crystal conductivities of both Ni(TBP)I and Ni(Pc)I in the region of 300–30 K is shown in Figure 5. Both compounds show

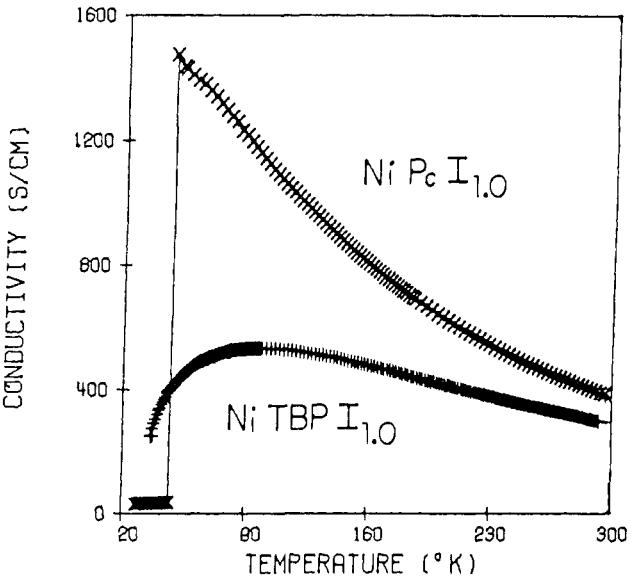


Figure 5. Temperature dependence of the single-crystal conductivity along the stacking axis for Ni(TBP)I and Ni(Pc)I.

a metal-like increase in conductivity upon cooling from room temperature, but the increase is more gradual for Ni(TBP)I than for Ni(Pc)I. The major difference in the temperature dependence of the conductivity for these compounds occurs at lower temperatures. The conductivity for Ni(TBP)I reaches a broad maximum before falling off rapidly. The Ni(TBP)I samples can be cycled repeatedly through this temperature region without any degradation in the conductivity. The conductivity maximum, $\sigma_\parallel{}^m$, comes at a temperature $T_m$ which ranges from 120 to 185 K depending on the crystal, with the higher conducting samples having a lower value of $T_m$. The highest conducting crystals, and therefore presumably the most perfect, reach a maximum in conductivity of $\sim$600 S cm$^{-1}$ at $T_m \approx 95$ K. In contrast, the conductivity of Ni(Pc)I increases with decreasing temperature until it reaches a maximum value of $\sim$1500 S cm$^{-1}$ at ca. 55 K but undergoes a discontinuous transition to a semiconducting state with further cooling.

An insight into the nature of the charge transport can be obtained by calculating the carrier mean free path along the stacking direction $\lambda_\parallel$

$$\lambda_\parallel = hA\sigma_\parallel/4e^2 \quad (7)$$

where $h$ is Planck's constant, $A$ is the cross-sectional area per conducting stack, and $e$ is the electronic charge.[8,45] At room temperature, $\lambda_\parallel$ ranges from 2.1 to 4.3 Å for Ni(TBP)I or from 0.66 to 1.3 times the intermolecular spacing, $d = c/2$. Since a value of $\lambda_\parallel/d$ less than unity is usually indicative of diffusive or hopping motion of charge carriers, while a value of $\lambda_\parallel/d$ greater than unity is associated with a wave-like mechanism for the conductivity, the room-temperature charge transport in Ni(TBP)I cannot be characterized by an idealized, limiting picture. The compound Ni(Pc)I shows a comparable mean free pathlength, ranging from 1.0 to 2.3 intermolecular spacings.[1c] Other molecular crystals exhibiting metal-like behavior ($d\sigma/dT < 0$ where $T > T_m$) have been found with $\lambda_\parallel/d > 1$, such as $TTT_2I_3$ (2.1–2.8)[46] and HMTSF–TCNQ (1.6–2.5),[47] as well as with $\lambda_\parallel/d < 1$, such as TTF–TCNQ (0.4–0.6),[48] $K_2Pt(CN)_2Br_{0.3}\cdot 3H_2O$ (0.6),[8c] and Ni(OMTBP)$I_{1.08}$ (0.04).[2b]

(42) Elliot, R. J.; Gibson, A. F. "An Introduction to Solid State Physics and its Applications"; Macmillan Press: London, 1974, p 437.
(43) Torrance, J. B.; Tomkiewicz, Y.; Silverman, B. D. *Phys. Rev. B* **1977**, *15*, 4738–4749.
(44) (a) Delhaes, P.; Coulon, C.; Flandrois, S.; Hilti, B.; Mayer, C. W.; Rihs, G.; Rivory, J. *J. Chem. Phys.* **1980**, *73*, 1452–1463. (b) Somoano, R. B.; Yen, S. P. S.; Hadek, V.; Khanna, S. K.; Novotny, M.; Datta, T.; Hermann, A. M.; Woollam, J. A. *Phys. Rev. B* **1978**, *17*, 2853–2857.
(45) Mott, N. F.; Davis, E. A. "Electronic Processes in Noncrystalline Materials"; Clarendon Press: Oxford, 1971.
(46) Isett, L. C.; Perez-Albuerne, E. A. *Solid State Commun.* **1977**, *21*, 433–435.
(47) (a) Bloch, A. N.; Cowan, D. O.; Beckgaard, K.; Pyle, R. E.; Banks, R. H.; Poehler, T. O. *Phys. Rev. Lett.* **1975**, *34*, 1561–1564. (b) Greene, R. L.; Mayerle, J. J.; Schumaker, R.; Castro, G.; Chaikin, P. M.; Etemad, S.; La Placa, S. J. *Solid State Commun.* **1976**, *20*, 943–946.
(48) Etemad, S.; Engler, E. M.; Schultz, T. D.; Penney, T.; Scott, B. A. *Phys. Rev. B* **1978**, *17*, 513–528.

The temperature dependence of the conductivity for Ni(TBP)I is similar to that found both in metal-based conductors such as the TCP salts and in several good organic conductors such as NMP-TCNQ.[8] Epstein and Conwell[49] have presented an equation for $\sigma(T)$ which incorporates a Boltzmann-like activation term and a temperature-dependent preexponential.

$$\sigma(T) = AT^{-\alpha} \exp(-\Delta_0/kT) \quad (8)$$

A least-squares fit of the data in Figure 5 yields $A = 3.9 \times 10^5$, $\alpha = 1.17$, and $\Delta_0/k = 108$ K for the Ni(TBP)I crystal and satisfactorily reproduces the conductivity both in the high-temperature metallic region ($T > T_m$) and in the low-temperature semiconducting region ($T < T_m$). In general, the Ni(TBP)I crystals with the higher values of $\sigma_\parallel^m$ are best described by eq 8, but data from almost all samples may be fit with an error of less than 3%.[50] The variation of $A$ from crystal to crystal is large, presumably reflecting variations in crystal quality, but $\alpha$ and $\Delta_0/k$ are essentially constants. In contrast, the conductivity curves for Ni(Pc)I for $T > 55$ K can be described formally by an equation like eq 8 for $\alpha = 1.9$, but only with $\Delta_0 = 0$. We are unaware of a similar analysis of the TCP data, but in several organic conductors $\alpha$ ranges from 2 to 4 with $\Delta_0/k$ ranging from 350 to 1400 K,[49,51] while for the Ni(OMTBP)$I_{1.08}$ species, $\alpha = 2.87$ and $\Delta_0/k = 900$ K.[3b] An analysis of only the low temperature region of the KCP[10] compound yields an activation of $\Delta_0/k = 660$ K.[52]

Epstein and Conwell[49] originally applied their analysis to the NMP-TCNQ system, where they ascribed the Boltzmann term to an activated generation of charge carriers in a narrow-bandgap semiconductor and the pre-exponential term to a temperature-dependent mobility. However, this interpretation predicts that the magnetic susceptibility should show an activated temperature dependence, which is not observed for Ni(TBP)I or for Ni(OMTBP)$I_{1.08}$, whose conductivity data were also fit to eq 8. The conductivity for Ni(OMTBP)$I_{1.08}$ was interpreted[3] in terms of the atomic limit of a partially oxidized material in which weak intrastack interactions can nonetheless give high conductivities. Charge transport occurs by diffusive motion of polarons with the activation energy, $\Delta_0$, associated with the polaron binding energy. This limiting case, however, is associated with a Curie law dependence of the magnetic susceptibility, again contrary to observation for Ni(TBP)I.

Alternatively, the general features of the temperature dependence of the conductivity might be described by models based on the effects of disorder, impurities, and imperfections found in real crystals. Structural disorder such as that of the triiodide chains of Ni(TBP)I generates random potentials. It has been suggested[53] that this can localize the carrier states in a one-dimensional crystal,[54] and the predicted[55] temperature dependence of $\sigma(T)$ is in qualitative accord with the results for Ni(TBP)I (Figure 5). This mechanism cannot be ruled out on the basis of the magnetic data since a roughly temperature-independent susceptibility at temperatures above $T_m$ is consistent with the model. However, there is no evidence that this mechanism contributes to the conductivity of Ni(Pc)I in which disorder of the triiodide chains also occurs, and we thus suggest that the mechanism does not dominate the conductivity of Ni(TBP)I.

Alternatively, impurities and crystal imperfections can also localize electronic states by creating breaks in the conducting chains.[56] At high temperatures the conductivity within the model is metal-like, being controlled by intrastrand properties. At low temperatures $\sigma$(T) is governed by phonon-modulated tunneling[57] or hopping[56] past the interruption or between stacks, with a resulting activated dependence. The overall agreement with the observed temperature dependence of $\sigma$ along with the joint variability of $\sigma_m$ and $T_m$ from crystal to crystal, as noted above, suggests that this model may be important in describing charge transport in Ni(TBP)I. In any event, the intrinsic charge transport properties of Ni(TBP)I and Ni(Pc)I appear to differ significantly. Of the many Ni(Pc)I crystal examined from many different preparations, none showed a rounded conductivity maximum. In contrast, none of the Ni(TBP)I crystals exhibit the sharp transition observed in Ni(Pc)I.

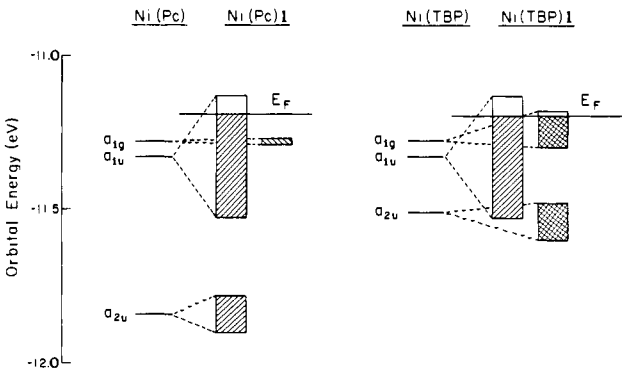


Figure 6. Schematic energy level diagrams for the highest occupied molecular orbitals of the parent metallomacrocycles and for the one-dimensional bands in the M(L)I molecular conductors. The shading, (//) and (\\), denotes ligand- and metal-centered bands, respectively. Crosshatching denotes bands of mixed character: left, Ni(Pc) and Ni(Pc)I; right, Ni(TBP) and Ni(TBP)I. The approximate energies of the Ni(Pc) molecular orbitals are taken from ref 58. The $a_{1u}$ and $a_{1g}$ ($d_{z^2}$) orbitals of Ni(TBP) are arbitrarily given the same energies as those for Ni(Pc), and the energy of $a_{2u}$ is approximated following ref 41 and 58. The $a_{1u}$ bandwidths are suggested by the susceptibility results, and other widths are scaled according to intermolecular overlaps.[41]

## Discussion

We have synthesized two highly conducting molecular solids, Ni(Pc)$I_{1.0}$[1] and Ni(TBP)$I_{1.0}$. The compounds are prepared from metallomacrocycles with different electronic properties[36] yet have identical crystal structures and identical ionicity (degree of partial oxidation). This provides a unique opportunity to relate the magnetic and charge-transport properties of a M(L)I solid to the electronic structure of the fundamental building blocks, with all other factors held constant.

The magnitude of the room-temperature single-crystal conductivity along the tetragonal axis is nearly identical for both Ni(TBP)I and Ni(Pc)I and places both compounds relatively high in the range of conductivities for molecular metals. The two partially oxidized materials exhibit similar low and roughly temperature independent magnetic susceptibilities. The reduction of the susceptibilities from the value of $^1/_3$ spins/macrocycle expected on the basis of the ionicity is indicative of equivalent, strong intrastack intermolecular interactions in the two systems and corresponds to one-dimensional, tight-binding bandwidths of roughly 0.4 eV. However, the similarity in the strength of the intermolecular interaction does not extend to the properties of the carriers themselves. The details of the charge-transport processes in the two materials are different since the temperature dependences of the conductivity for the two compounds show little similarity. The striking differences in the EPR $g$ values and line widths, as well as in their temperature dependence, arise from corresponding differences in the nature of the "hole" species created by the oxidation. We now show that the observed differences between Ni(Pc)I and Ni(TBP)I can be understood within the generally accepted model for the electronic structure of the

(49) Epstein, A. J.; Conwell, E. M.; Sandman, D. J.; Miller, J. S. *Solid State Commun.* **1977**, *23*, 355–358.
(50) Based on the rms deviation calculated from the fit.
(51) Epstein, A. J. In ref 8a, pp 155–160.
(52) Underhill, A. E.; Wood, D. J. In ref 8a, pp 516–524.
(53) Megtert, S.; Pouget, J. P.; Comès, R. In ref 8i, pp 196–201.
(54) Borland, R. E. *Proc. Phys. Soc. London* **1961**, *78*, 926–931.
(55) (a) Bloch, A. N.; Weisman, R. B.; Varma, C. M. *Phys. Rev. Lett.* **1972**, *28*, 753–756. Gruner, G.; Janossy, A.; Holczer, K.; Mihaly, G. In ref 8i, pp 246–254. (c) Epstein, A. J.; Miller, J. S. In ref 8i, pp 265–272. (d) Epstein, A. J.; Conwell, E.; Miller, J. S. In ref 8a, pp 183–208.
(56) (a) Kuse, D.; Zeller, H. R. *Phys. Rev. Lett.* **1971**, *27*, 1060–1063. (b) Rice, M. J. *Phys. Lett. A* **1972**, *39*, 289–290. (c) Rice, M. J.; Bernasconi, J. *Phys. Lett.* **1972**, *38*, 277–278. (d) Rice, M. J.; Bernasconi, J. *J. Phys. F* **1973**, *3*, 55–66.
(57) (a) Sheng, P.; Sichel, E. K.; Gittleman, J. I. *Phys. Rev. Lett.* **1978**, *40*, 1197–1200. (b) Sheng, P. *Phys. Rev. B* **1980**, *21*, 2180–2195.

porphyrin-like metallomacrocycle subunits.[36,58]

For both of the parent complexes, the highest occupied ligand or molecular orbital is of $a_{1u}$ symmetry, and the next highest is of $a_{2u}$ symmetry. For Ni(Pc) there is a sizable energy gap between the two MO's (Figure 6).[58] The highest occupied metal orbital of Ni(Pc), $d_{z^2}$, must be nearly degenerate with the highest occupied ligand $\pi$ ($a_{1u}$) orbital, since separate electrochemical oxidations are not observed[59] for metal and ligand and since a change in the environment of the Ni(Pc) cation can invert the relative ordering of these orbitals. The substitution of the bridging nitrogen atoms of a phthalocyanine with less electronegative methine carbon atoms to form a tetrabenzoporphyrin almost certainly leaves the $a_{1u}$ and $d_{z^2}$ orbitals nearly degenerate[39] but significantly reduces the energy gap between the ligand $a_{1u}$ and $a_{2u}$ MO's,[36] because the energy of the $a_{2u}$ orbital increases. Thus, the three highest occupied MO's of a Ni(TBP) subunit are of very comparable energy (Figure 6).

The metal-over-metal stacking arrangement in the crystals of these two Ni(L) compounds is ideal for intermolecular interactions between the $a_{1u}$ ligand $\pi$ molecular orbital and between the metal $d_{z^2}$ orbitals; mixing between the $a_{1u}$ and $d_{z^2}$ orbitals is forbidden by symmetry, however.[60] Such interactions generate the large effective one-dimensional bandwidths which are calculated from the magnetic susceptibility. Starting from the Ni(Pc) energy level diagram of Figure 6, the conclusion, based on the $g$ value analysis, that the charge carriers of Ni(Pc)I are ligand centered, leads to a simple picture in which the oxidation of Ni(Pc) occurs exclusively from the ligand-centered $a_{1u}$ band, with the top edge of the $d_{z^2}$ band required to lie at least 3 kT below the Fermi level. Thus, this material could well be included in the class of organic $\pi$ conductors, with the metal ion acting as a substituent to modify the electronic properties of the $\pi$-system.

In contrast, the electronic structure of a Ni(TBP) stack is more complicated. The near degeneracy of the three highest filled molecular orbitals on the parent complex can, under the influence of intrastack interactions, lead to the formation of three overlapping bands. Although the three molecular states transform independently under the $D_{4h}$ molecular symmetry and do not mix quantum mechanically, in a Ni(TBP) stack the ligand $a_{2u}$ MO and metal $d_{z^2}$ orbital can hybridize through the influence of intermolecular interactions.[60] Thus, the result of the intrastack interactions is a one-dimensional band structure with a single pure $\pi$ band and two $\pi$-d hybridized bands, with the one of greater d character being raised in energy by the interactions (Figure 6).

The conclusion that the Ni(TBP)I charge carriers show a mixed ligand $\pi$, metal d character might mean either that the oxidation occurs from a hybridized band or that oxidation occurs from two bands, one of pure ligand $\pi$ ($a_{1u}$) and the other largely of $d_{z^2}$ character. In the second case, the $g$ factor decomposition given above becomes equivalent to that performed on the two-stack conductors such as TTF-TCNQ;[61] the coefficients $\gamma^2$ and $\beta^2$ would represent the relative susceptibilities of the ligand $\pi$ and metal d bands, not necessarily the relative spin densities on ligand and metal. We show elsewhere[41,62] that the temperature dependence of the $g$ values requires the involvement of carriers associated with two independent bands. As a consequence, the observation of a single EPR line for Ni(TBP)I requires carrier interchange between these bands to occur with a frequency, $\omega_i$, which is large with respect to the frequency difference between the resonance frequency for a pure metal d spin and a pure ligand $\pi$ radical (i.e., $\omega_i > \beta(g_{Ni} - g_L)H_0/h \approx 10^9$–$10^{10}$ s$^{-1}$). In molecular terms, the $[Ni(TBP)]^+$ cation exhibits a second form of mixed valency, or electronic tautomerism, with interconversion between the $[Ni^{III}(TBP)]$ and $[Ni^{II}(TBP)^+]$ forms occurring at a frequency $\omega_i$.[63]

In addition, charge carriers move along a Ni(TBP) stack giving the observed charge transport. The small metal–metal overlap for the Ni $d_{z^2}$ orbitals even at the small observed separation suggests that the $[Ni^{III}(TBP)]$ tautomer represents a temporary trap. In this case the reduced low temperature conductivity of Ni(TBP)I, as compared with Ni(Pc)I, may be a consequence of the observed increase in the metal character of the Ni(TBP)I carriers. The multiple band character of the charge carriers will tend to suppress Peierls distortions and may thus in and of itself account for the suppression in Ni(TBP)I of the sharp metal–semiconductor transition seen in Ni(Pc)I.

## Summary

A comparison of the two isostructural and isovalent compounds, (phthalocyaninato)nickel iodide and (tetrabenzoporphyrinato)-nickel iodide, has been made. Both molecular solids show strong intrastack interactions and high conductivity, but the exact nature of the band structure, and therefore the conductivity, is sensitive to the electronic properties of the molecular subunits. Comparisons between systems of these types are important because they allow us to probe the effect of small electronic changes in the subunits on the magnetic and charge-transport properties without variations in the ionicity and crystal structure of the partially oxidized solid. As a consequence of this procedure, we have discovered the first clear example of a doubly mixed valence conductive molecular solid, Ni(TBP)I.

**Acknowledgment.** We thank Dr. William B. Euler and Dr. Charles J. Schramm for helpful discussions and Dr. James E. Roberts for 12-GHz EPR spectra. This work has been supported under the NSF-MRL program through the Materials Research Center of Northwestern University (Grant DMR79-23573) (J.M.) and by National Science Foundation Grants DMR77-26409 (T.E.P.) to B.M.H. and CHE80-09671 to J.A.I. L.J.P. acknowledges receipt of an NSF Graduate Fellowship.

**Supplementary Material Available:** The listing of observed and calculated structure amplitudes and Table III, the root-mean-square amplitudes of vibration (5 pages). Ordering information is given on any current masthead page.

(58) Schaffer, A. M.; Gouterman, M.; Davidson, E. R. *Theor. Chim. Acta* **1973**, *30*, 9–30.

(59) Manassen, J.; Bar-Ilan, A. *J. Catal.* **1970**, *17*, 86–92.

(60) Although the site symmetry in the lattice of a Ni(TBP) unit is $C_{4h}$, the orbitals on a unit transform under the full lattice symmetry of $D_{4h}^2$ ($P_4/mcc$). In the notation of Miller and Love (Miller, S. L.; Love, W. F. "Tables of Irreducible Representations of Space Groups and Co-Representations of Magnetic Space Groups"; Pruett Press: Boulder, CO, 1967), for the reciprocal lattice vector along the stacking axis, $k_z$, equal to zero, the ligand molecular orbitals of $a_{1u}$ ($D_{4h}$) and $a_{2u}$ symmetry transform as $\Gamma_1^-$ and $\Gamma_3^-$, respectively, while the metal $d_{z^2}$ orbital ($a_{1g}$ in $D_{4h}$) transforms as $\Gamma_1^+$. However, for $0 < k_z < \pi/c$, the ligand $a_{2u}$ MO and the metal $a_{1g}$ orbital can mix because they both transform as $\Lambda_1$; the ligand $a_{1u}$ MO cannot mix with the other two since it transforms as $\Lambda_4$.

(61) Tomkiewicz, Y.; Scott, B. A.; Tao, L. J.; Title, R. S. *Phys. Rev. Lett.* **1974**, *32*, 1363–1366.

(62) Euler, W. B.; Martinsen, J.; Pace, L. J.; Hoffman, B. M.; Ibers, J. A. *Mol. Cryst. Liq. Cryst.*, in press.

(63) The absence of d character in the carrier spins of $Ni(OMTBP)I_{1.08}$[2b] indicates how subtle is the balance of factors which leads to this novel phenomenon. Molecular orbital calculations[41] show that the electronic effect of the Ni(OMTBP) methyl substituents is to raise slightly the energy of the TBP $a_{1u}$ orbital; apparently, this is enough to suppress oxidation to a state with $d_{z^2}$ character.